Reports

Triton's Geyser-Like Plumes: Discovery and Basic Characterization

L. A. Soderblom, S. W. Kieffer, T. L. Becker, R. H. Brown, A. F. Cook II, C. J. Hansen, T. V. Johnson, R. L. Kirk, E. M. Shoemaker

At least four active geyser-like eruptions were discovered in Voyager 2 images of Triton, Neptune's large satellite. The two best documented eruptions occur as columns of dark material rising to an altitude of about 8 kilometers where dark clouds of material are left suspended to drift downwind over 100 kilometers. The radii of the rising columns appear to be in the range of several tens of meters to a kilometer. One model for the mechanism to drive the plumes involves heating of nitrogen ice in a sub-surface greenhouse environment; nitrogen gas pressurized by the solar heating explosively vents to the surface carrying clouds of ice and dark particles into the atmosphere. A temperature increase of less than 4 kelvins above the ambient surface value of 38 ± 3 kelvins is more than adequate to drive the plumes to an 8-kilometer altitude. The mass flux in the trailing clouds is estimated to consist of up to 10 kilograms of fine dark particles per second or twice as much nitrogen ice and perhaps several hundred or more kilograms of nitrogen gas per second. Each eruption may last a year or more, during which on the order of a tenth of a cubic kilometer of ice is sublimed.

V OYAGER 2 DISCOVERED GEYSER-like (1) plumes erupting from the surface of Neptune's large retrograde satellite, Triton (2). The basic observations and characteristics of the plumes are described here. Our purpose is to document the scale, geometry, optical properties, and temporal behavior of the eruptions; to estimate some other properties from the observations (eruption duration, wind velocities, particle properties, cloud properties, and mass fluxes); and to discuss simple constraints (energy requirements, solar input, total erupted mass, implications for wind circulation models) that are important for other analyses.

During the years prior to Voyager 2's historic encounter with the Neptune System, it was speculated that Triton could have exotic, active surface processes. Earth-based telescopic data showed absorptions due to methane and possibly to nitrogen in Triton's surface reflection spectrum (3). The molecular nitrogen absorption feature detected at 2.15 μm is usually such a weak

L. A. Soderblom, T. L. Becker, R. L. Kirk, E. M. Shoemaker, U.S. Geological Survey, Flagstaff, AZ 86001.
S. W. Kieffer, Arizona State University, Tempe, AZ 85287.
R. H. Brown, C. J. Hansen, T. V. Johnson, Jet Propulsion Laboratory, California Institute of Technology, Pasadena, CA 91109.
A. F. Cook II, Harvard-Smithsonian Center for Astrophysics, Cambridge, MA 02138.

feature that in this case a substantial amount of nitrogen was suspected, in fact a path length equivalent to a meter or more of solid N_2. As we discuss here and in companion reports (4), such a thick surface layer has interesting ramifications for understanding the observed eruptions.

The presence of these volatiles, possibly in substantial quantity, led to a range of speculation as to what Triton's surface environment might be like. Prior to the Voyager encounter Triton's diameter, and hence the albedo of its surface, were poorly known. It was possible that if Triton's diameter were large and its albedo very low, its surface temperature might exceed the triple point temperature for N_2 ($\sim$63 K). If so, a range of exotic phenomena—nitrogen rivers, lakes, rain, and snow—could be imagined. As Voyager 2 drew close to Triton during the last few weeks prior to the encounter, the data showed its diameter to be near the minimum possible and its albedo to be extremely high (with a Bond albedo in excess of 0.7) (2). This promised an extremely cold surface environment: in fact, measurement showed a surface of nearly globally uniform temperature of 38 ± 4 K and a dominantly N_2 atmosphere with a pressure of 16 ± 3 μbar (5). The likelihood of active surface phenomena under these conditions seemed low indeed.

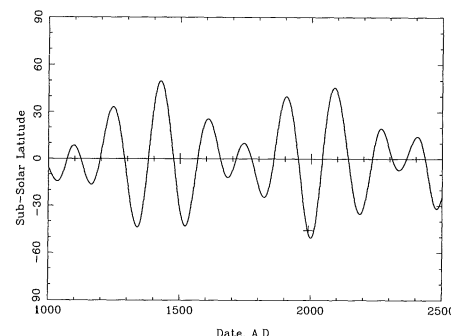Although Triton's geyser-like eruptions

Fig. 1. Seasonal excursion of the sub-solar latitude on Triton. Figure taken from Cruikshank and Brown which was derived from work of Harris (8).

were not actually identified until a month after Voyager 2's encounter, some form of surface activity was suspected immediately after the closeup images were acquired. These images showed slightly darker streaks superposed on Triton's extensive, bright south polar cap, a cap that was actively subliming and would continue to do so during the next several decades while Triton's southern summer continued.

The existence of dark material at the surface of Triton was not particularly surprising. As already mentioned, methane was known to exist at the surface and in the atmosphere. A range of energetic processes (cosmic ray bombardment, ultraviolet-photolysis, charged particle bombardment) are known to generate organic polymers from methane (6). Alternatively, dark particles could be remnants of primordial dark hydrocarbons (such as those found in cometary nuclei) that accreted onto Triton's surface. In either case such particles would act as neutral, non-volatile fragments, to be mixed with and transported along with the volatile materials.

It seemed unlikely that the myriad of dark streaks could survive multiple Triton years (each equal to 165 Earth years) while the polar volatiles migrated from pole to pole seasonally. In fact, the streaks seemed likely to be younger than a Triton year. The combination of Triton's rapid orbital precession ($\sim$688 years) (7) and Neptune's orbital period causes the seasonal excursion of the sub-solar latitude to vary wildly from one Triton year to the next (Fig. 1) (8). In some Triton years the sub-solar point gets no farther than about 10° from the equator; in others the latitude of solar zenith can reach as high as 52°. The current Triton southern summer is an exceptionally hot one; the solar latitude is about 45°S. Solstice will occur in about 10 years with a sub-solar latitude of about 52°S; the sun will remain at high southerly latitude for several decades. The last time the southern summer solstice reached this far south was about

A.D. 1350 (Fig. 1). It is conceivable that the streaks are embedded in the ice layers and exposed by deep sublimation of the ice during the currently excessively hot summer. Thus, the streaks could be as old as a few hundred years, dating back to the time the ice had been sublimed to below its current depth. Nonetheless, the streaks still would be extremely young on a geologic time scale.

The youthful nature of the streaks and the absence of obvious eruptive phenomena led Sagan and Chyba (9) to examine a model in which the streaks were created as wind-blown debris strewn over the subliming ice. They concluded this to be conceivable if the fine particles were virtually cohesionless. Although discovery of the erupting geysers obviates the need for saltation to pick material up, Sagan and Chyba also examined in some detail the question of suspension of fine particles in Triton's near-vacuum atmosphere. That aspect of their work was valuable here in deriving the physical character-istics of the plumes and their cloud trails, in particular, for estimating mass fluxes.

The collective northeast alignment of most of the streaks suggested that winds in Triton's atmosphere were in some way implicated in the formation of Triton's streaks. The sublimation-driven winds would naturally move northward out of the south polar region, deflected to the east by Triton's slow rotation. Although the preponderance of the streaks are so aligned, trending to the northeast, others are aligned in different directions (10). The issue was not whether Triton's winds had carried suspended material downwind, but how the material became suspended in the first place: by wind alone, as Saga and Chyba argued was in fact possible, or by some eruptive phenomenon.

Soon after the encounter we examined the possibility of solar-driven venting of nitrogen ice and gas that could entrain dark particles, injecting them into the global winds. Details of such models are elaborated more fully in this issue (3) and by Yelle et al.

(11). In these models sunlight is absorbed by dark particles encased in the nitrogen ice layer which acts as a greenhouse, raising the temperature and increasing the pressure of N_2 gas which would eventually exhaust from vents carrying dark particles aloft. Our conclusion was that such processes are in fact quite feasible and might be a plausible explanation for injecting material into the wind. Coupled with the fact that numerous discrete clouds are visible in images, this gave us impetus to search the data for evidence of eruptions from the surface.

The most sensitive method to search for material aloft over the illuminated disk (as opposed to limb and terminator images) is to use anaglyphic composites. The process involves establishing precise geodetic correspondence between two images that have strong stereoscopic separation. These are projected onto a model of the planet's surface, in this case a sphere, and composited in different colors. Figure 2 shows the anaglyphic composite in which the geysers were actually discovered. Most of the features which do in fact lie on the surface register in the composite, but a few (visible as red-blue pairs or fringes) clearly do not as they are above the surface. The easiest to see is the marked plume "W" in Fig. 2 (where a red streak is below a blue one). Examination of these areas shows such features to be clouds of material above the ground. In two cases dark stems or columns can be seen rising directly from the surface into the clouds above; these are informally referred to as "east" and "west" plumes. East plume is seen to be one of a cluster of eruptions. At least two other companions are visible a few tens of kilometers farther to the south (up in Fig. 2). Although rising columns connecting these companions to the surface are not visible, their similarity to the more obvious plumes suggests that they are eruptions from the surface, rather than simply atmospheric condensates.

The two well-observed plumes are south of the present subsolar latitude of (45°S) in the region currently in continuous sunlight (west plume at 49°S and east plume at 57°S). Each plume was imaged multiple times; albeit some of the images have marginal resolution to see the plumes clearly. Table 1 summarizes the available Voyager imaging observations. The best three views of each of the plumes are shown in Figs. 3 and 4. In both cases the plume columns rise into small, dark, dense clouds at their tops where they join long, horizontal, diffuse dark clouds which trail off nearly due west (to the right in Figs. 3 and 4). In the last two, best images of each plume (bottom images), the rising columns appear to slightly overshoot the height of the trailing cloud
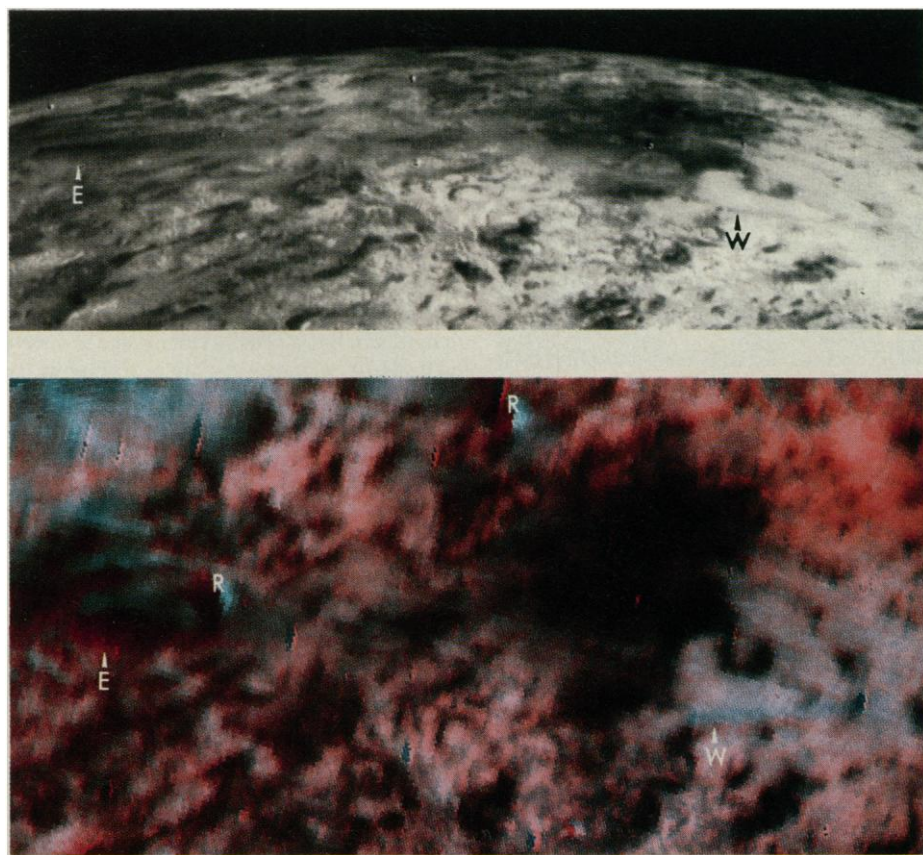

Fig. 2. Voyager 2 images of the south polar region of Triton in which the geyser-like eruptions were discovered. In the top image (11394.01) the plumes are viewed at high-emission angles with east plume (E) at 75.0° and west plume (W) at 66.7° (see Table 1). A second image (11387.09) (used as the blue-green component in the bottom view) shows the two plumes at much lower emission angles (east ~52.8°, west ~37.0°). Both images were projected to an orthographic projection centered at 0°E and 15°S (approximately the sub-spacecraft position for the lower emission angle view) and composited in color (with 11394.01 in red and 11387.09 in blue-green). Two large reseaux (R) are marked in the composite; numerous smaller blemishes are unmarked. The plumes are detectable as paired red-blue features or fringes. West plume (W) is the easiest to identify. East plume (E) is parallel to two other apparent eruptions (seen just above it, or to the south).

by about the resolution of the images or about 1 km. Because the geyser-like columns and clouds that trail downwind from them are well above the surface, parallax causes the features to shift in position from view to view. The top of the west plume column and its trailing cloud are both estimated from the parallax to be 8 ± 1 km above the surface. Due to its diffuse character, the height of east plume and altitude of its cloud are more difficult to measure but they are also in the range of 8 km.

The plumes are generally quite low in contrast. For instance, the surface region against which west plume is seen, has a brightness between 0.7 to 0.8 relative to that for a unit reflecting Lambertian target illuminated normal to its surface. The plume and cloud trail show typical brightness of 0.63 to 0.65; the darkest parts being the small dark patch on the surface from which the column rises and the small dark cloud at the top of the column which have brightnesses of 0.59.

In all three views of west plume, the shadow of the cloud trail can be recognized. The sun was nearly overhead as the plume was only about 10° from the sub-solar point (see Table 1). Measurement of the separation of the shadow from the cloud gives an independent confirmation of the roughly 8-km altitude of the top of the plume and trailing cloud. Figure 5 is a stereo pair generated from the two last (and highest resolution) images of the west plume; they have been projected to a common surface coordinate system to remove the excessive aspect distortions to allow easier stereoscopic viewing.

Of the two plumes, the east plume shows a broader, denser trailing cloud, fanning out and extending over 100 km downwind. There is no clear evidence of variability in the density or extent of its cloud. In contrast, the trailing cloud of the west plume appears to have changed in several ways. First, it increased both in length and density during acquisition of the views in Fig. 3 (which were acquired about 45 min apart); apparently its length roughly doubled from ~80 km to over 150 km. This change in length implies a wind velocity at the 8-km altitude of ~15 m s^{-1}. The morphology of the cloud trail also changed. In the first two views of Fig. 3 the cloud trail is seen to be intermittent, consisting of two or three discrete small clouds separated by about 10 km; the shadows of these individual clouds are also visible. If our estimate of the wind velocity is reasonable, the eruption of west plume was intermittent on the time scale of 10 to 20 min.

A characteristic of the data compression scheme used on the spacecraft occasionally resulted in missing alternate lines. The third and highest resolution image of west plume (bottom, Fig. 3) suffered from this condition. Figure 6 (top), a raw, unaltered version of this image, shows every other line (manifested as vertical stripes) to be missing. The fact that it does not show the variable structure in the cloud visible in the first two views shown may be artificial.

The apparent narrowness of the west plume column in the bottom view of Fig. 3 is also introduced by the missing line artifact. Based on the other views, the apparent diameters of the rising columns are 2 to 3

Table 1. Voyager imaging observations of Triton geysers. East plume is located at 49°S and 2°E; west plume at 57°S and 38°E. Table values include the solar incidence angle at source (i), the emission angle at source (ϵ), and the resolution in kilometers per pixel (RES); SNR, signal-to-noise ratio.

| Frame ID-filter	West plume: 49°S, 2°E		East plume: 57°S, 38°E		RES	Comments
	i	ϵ	i	ϵ		
11386.39-orange					4.1	Low SNR
11386.51-blue					4.1	Moderate SNR
11386.57-violet	19.0	37.0	40.5	52.8	4.0	Moderate SNR
11387.03-green					4.0	Moderate SNR
11387.09-clear					4.0	Best of set
11387.15-UV					3.9	Low SNR
11393.03-clear					1.6	Best of set
11393.05-violet	11.2	62.4	33.9	72.4	1.6	Moderate SNR
11393.07-green					1.5	Moderate SNR
11394.01-clear	10.6	66.7	33.0	76.0	1.2	Best of both plumes
11394.11-clear	—	—	37.8	77.0	1.1	Missing lines
11395.03-clear	8.7	74.7	—	—	0.8	Missing lines
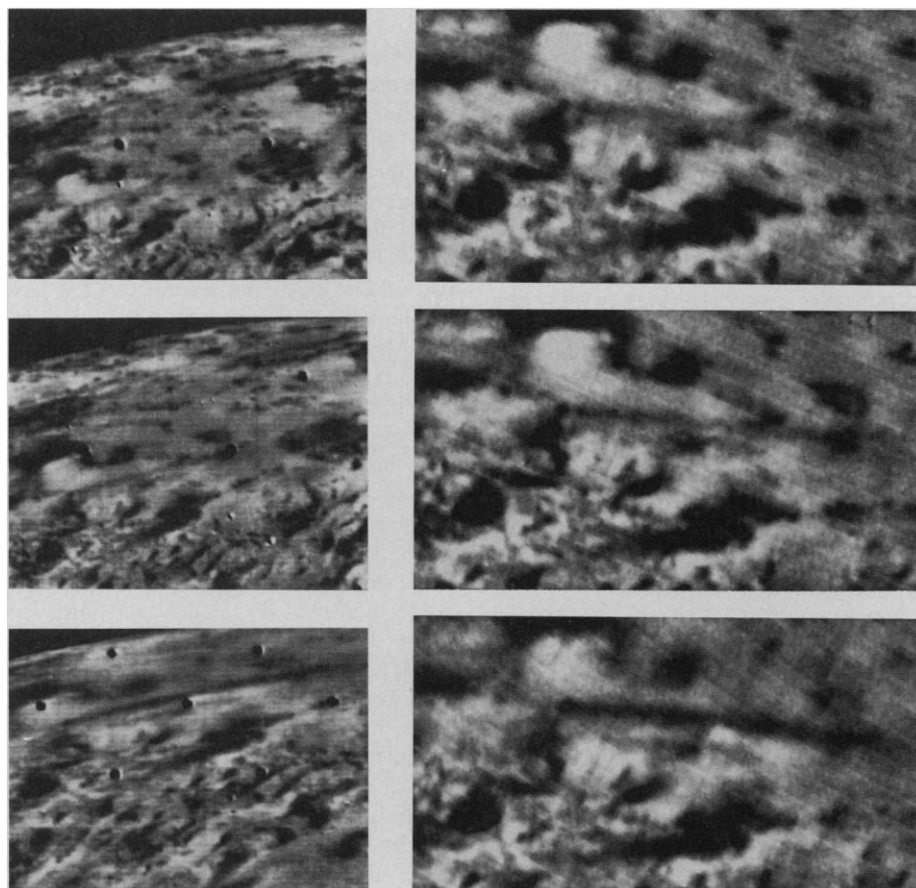
Fig. 3. Image set for west plume. The images shown from top to bottom are: 11393.03, 11394.01, and 11395.03 (see Table 1). The left-hand set of images has been left in the original spacecraft perspective, but printed a roughly uniform scale. Reseau marks have been left in left views. Images in the right-hand column have been projected onto a spherical surface with a viewing geometry similar to that of the top view on the left. Both sets have been spatially filtered to enhance detail.

km. The actual diameters of the column could be much smaller if they are surrounded by a descending sheath of material. The image of east plume in the bottom of Fig. 4 is the best example of what may be such a sheath.

The strongly enhanced image of Fig. 6 (bottom) shows that the clarity of the atmosphere changed at the latitude where the plumes occur. Above the cloud trail, south in that view, the atmosphere has a darker, murky appearance, whereas below the trail surface features are sharper and of higher contrast. This haze is evidently due to suspended particulates generated by the eruptions, distributed ubiquitously through the atmosphere to the south.

As already mentioned, most of the streaks on Triton's polar cap extend from what appear to be their sources to the northeast (2, 10). This is the direction that the Coriolis-deflected, sublimation-driven winds at the surface would naturally trend. The cloud trails of the two confirmed eruptions, however, trend due west. Ingersoll (12) has offered the attractive suggestion that Triton's polar winds have the following circulation pattern: At low altitude, within the Ekman boundary layer near the surface, the winds blow to the northeast in an anticyclone driven by the subliming cap. At higher altitudes, however, the circulation pattern is such that winds blow westward and southward, eventually descending into the bright, cold central polar region.

Given these ideas, a consistent model is that as a geyser reaches the final stages of eruption and begins to shut off, it erupts only a few kilometers or less in height. Then, the dark particles, carried to the northeast by the gentle surface winds in the boundary layer ($\sim$5 m s^{-1}, according to Ingersoll), have time to settle out onto the surface. By contrast, when the eruptions are fully developed, they reach the higher altitudes where the faster westward winds spread them widely, producing the murky atmosphere to the south.

Before discussing further analysis of the geyser observations, we introduce models for solar-driven nitrogen plume eruptions that have been suggested (2, 11) and are discussed elsewhere in this issue (4). In particular, these models suggest additional types of evidence that might be observable.

As described earlier, interpretation of a weak absorption feature in Triton's spectrum at 2.15 μm suggested that reflected sunlight penetrates roughly a meter of nitrogen over much of the surface (3). Dark organic polymers generated from methane are nonvolatile and would tend to collect at the base of the seasonally migrant layers of nitrogen ice. This situation could provide an extremely effective greenhouse, warming the ice in the subsurface. The vapor pressure of the N_2 ice increases extremely rapidly with increasing temperature; a temperature rise of only 4 K results in an order of magnitude increase in the pressure. If the ice layer were well enough annealed to form a seal, the vapor would migrate into porous reservoirs in the subsurface, charging the subsurface with pressurized nitrogen gas. If the pressurized gas encounters a vent or fracture through the seal, it will explosively decompress, launching a plume of material into the atmosphere. As the gas decompresses, a fraction will condense, forming nitrogen ice crystals; fine dark particles in the vicinity of the vent could easily be entrained in the gas as well.
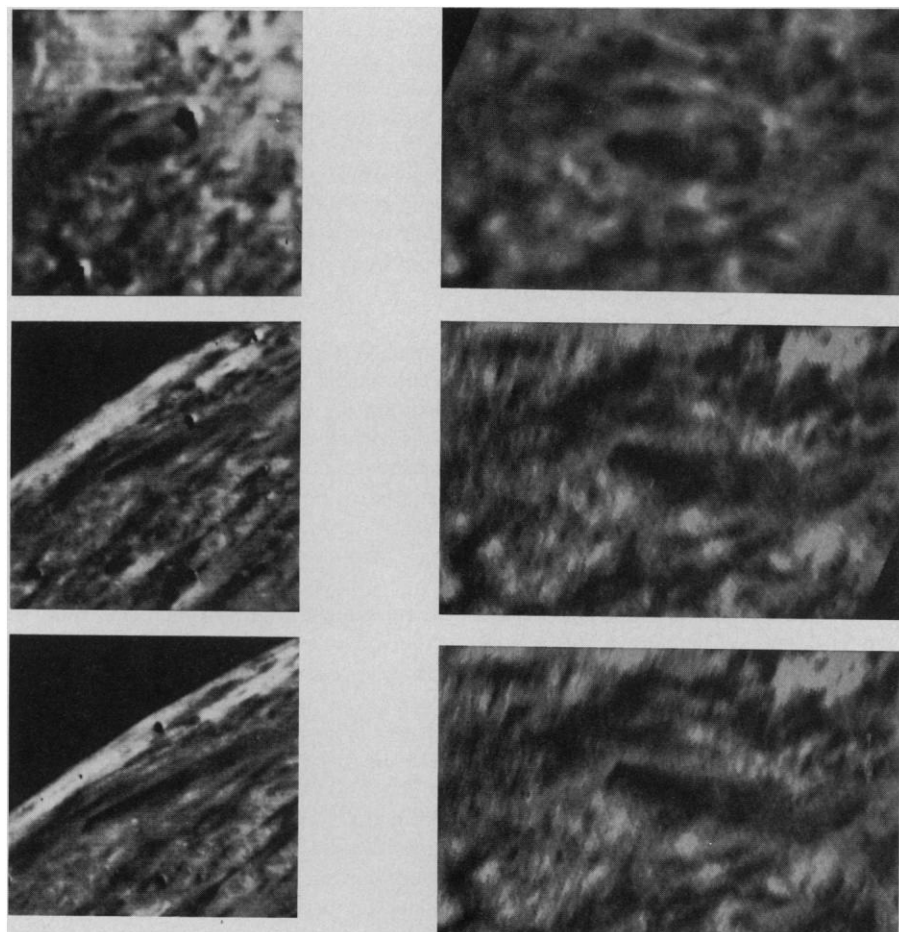

Fig. 4. Image set for east plume. From the top to bottom, the images shown are: 11387.09, 11393.03, and 11394.01 (see Table 1). Processing is the same as for Fig. 3.
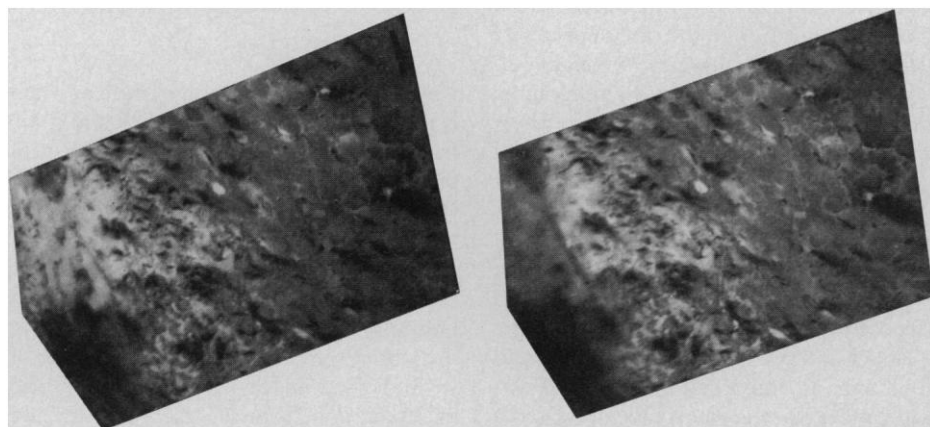

Fig. 5. Stereoscopic pair of west plume. Images 11394.01 and 11395.03 were projected onto a sphere centered at the equator. This was done to remove large aspect differences between the two to allow easier stereo viewing.
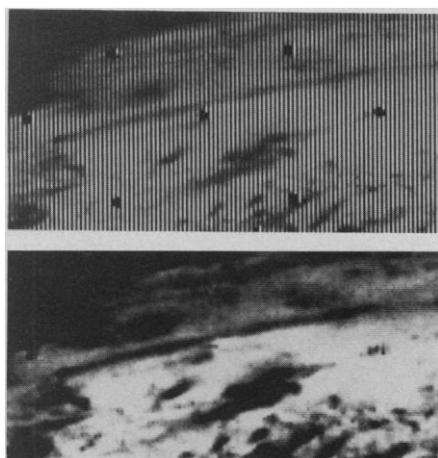
Fig. 6. Two versions of the highest resolution view of west plume (11395.03). (**Top**) The unaltered raw data with no interpolation of missing lines or reseau removal. (**Bottom**) Missing data has been interpolated, radiometric correction performed, and the contrast enhanced. No filtering or photometric fitting was done in this version so that relative brightnesses in the scene are faithfully preserved.

As the mixture rises, driven by momentum and possibly by positive buoyancy, it will be turbulently mixed with the atmosphere and eventually stop as it becomes neutrally or negatively buoyant. Not only must initial momentum and buoyancy (affected by loading with ice crystals and entrained dark particulates as well as by atmospheric entrainment) be considered in calculation of plume height, but fallout of the ice and particles as the plume rises is a dynamic process that continuously changes the buoyancy. Such fallout is suggested by what appears to be a sheath around east plumes (Fig. 4, bottom). Secondarily, heat transfer in the multiphase mixture must be considered in detailed calculations of plume height. Thus, in the next paragraph our intention is to indicate only that first-order models suggest that sufficient energy is available, even at the amazingly low surface temperature, to drive the geysers.

The velocity with which the plume is launched, its initial buoyancy, and the ratio of nitrogen gas to ice depends on the initial conditions of the gas reservoir. As it turns out, a very small increase in temperature, only a few degrees above the ambient of ~38 K, is sufficient to drive the observed phenomena. We give an example for vapor at an initial temperature of 42 K which undergoes isentropic decompression to an ambient temperature of 38 K (13). The original entropy for vapor at 42 K is 210.6 J mol^{-1} K^{-1}. As the mixture decompresses isentropically to 38 K, some fraction condenses to ice crystals. Vapor at 38 K has an entropy of 220.4 J mol^{-1} K^{-1}; ice at 38 K has an entropy of 38.4 J mol^{-1} K^{-1}. For

isentropic decompression

$$S_{42vapor} = (1 - x)S_{38vapor} + xS_{38solid} \quad (1)$$

where x is the mass fraction of ice crystals in the erupted plume. This equation yields 5.4% ice crystals at 38 K. The original enthalpy of the 42 K vapor is 8216 J mol^{-1}, whereas that for the erupted vapor is 8140.4 J mol^{-1} and for the ice is 971.7 J mol^{-1}. The change in enthalpy that is available to drive the eruption is

$$\Delta H = H_{42vapor} - (1 - x)H_{38vapor} - xH_{38solid} \quad (2)$$

which gives a change in enthalpy of 462.5 J mol^{-1}. If all of the enthalpy were converted to kinetic energy to accelerate the plume, the exit velocity would be 180 m s^{-1}. We estimate an initial velocity of only 100 m s^{-1} would in fact suffice to drive the plumes to 8 km, so in fact even lower temperature differences could drive the plumes. Yelle et al. (11) argue that the plumes might be largely convectively buoyant and a temperature difference of only about a degree is sufficient to launch plumes.

A case opposite to the positively buoyant plumes of Yelle et al. is that of a jet made negatively buoyant by the entrained solids (ice and dark particles) and driven against gravity by its initial momentum. An empirical model developed by Turner (14) relates the height of eruption to the fluxes of momentum and buoyancy into the jet. The maximum altitude that the jet will obtain can be expressed as follows:

$$x_m \approx 2u_0(\rho D/g\Delta\rho)^{1/2} \quad (3)$$

where D is the vent diameter, ρ is the density, u_0 the initial velocity, $\Delta\rho$ the density difference between the plume and the atmosphere (due to loading by the solid particles), and g the acceleration due to gravity (0.79 m s^{-2}). For the case discussed above (a 4 K temperature difference and an initial velocity of 180 m s^{-1}) with a mass fraction of solid assumed to be 0.1, the diameter of such a plume would have to be roughly 20 m to reach the observed 8-km altitude. From the density of Triton's atmosphere (roughly 10^{-4} kg m^{-3}), this would imply a mass flux of gas and particles of about 5 kg s^{-1}, which is on the low side of the reasonable range discussed below. The vent diameters of east and west plumes are therefore very roughly constrained between several tens of meters and several kilometers.

The optical properties of the plumes and cloud trails are important in estimating particle properties and the mass of material being transported in the plumes. In the case of west plume, for which the shadow is visible, the cloud trail is 5 to 10% darker

than Triton's extremely bright polar cap against which it is seen. The shadow of the cloud likewise reduces the brightness of the surface also by several percent. This is consistent with a cloud of fine particles consisting either of very dark (effectively black) dust with an optical depth of ~0.1 or nitrogen ice crystals with an optical depth perhaps 50% higher (or some intermediate mixture).

We can place a limit on the mass flux in the west plume cloud trail by noting that the dark particles remain suspended over the length of some 150 km. Sagan and Chyba (9) examined the settling speed for particles in Triton's sparse atmosphere. They noted that particles smaller than about 100 μm settle in the Epstein or kinetic regime, given Triton's atmospheric conditions. From their work we start with the following relationship:

$$V \approx 19.0 \, D_p(\rho/P) \quad (4)$$

where V is settling velocity (in meters per second) in a level of the atmosphere with pressure P (in Newtons per square meter) for a particle of diameter D_p (in meters) and density ρ (in kilograms per cubic meter). We can place a limit on the settling velocity for the west plume cloud trail:

$$V < u\Delta h/L \quad (5)$$

where L is the length of the cloud trail, u is the wind velocity, and Δh is the maximum distance settled from the initial 8-km height. Because we detect no significant change in cloud elevation over the 150-km length, we take Δh to be 1 km, roughly the precision with which we can estimate the altitude. From our own direct estimate or from Ingersoll's circulation model (12), reasonable wind velocities are 10 to 20 m s^{-1}, so an upper limit for the settling velocity is roughly 0.1 m s^{-1}. This corresponds to a particle diameter of ~5 μm for the pressure at 8 km (about 0.9 N m^{-2} and particles with a density of 10^3 kg m^{-3}). The mass flux of particles in the cloud trail is simply

$$M_F = 2 \, D_p \, \rho \, \tau w u/3 \quad (6)$$

where τ is the optical depth of the cloud and w its width. Combining Eqs. 4, 5, and 6, we have an expression which is independent of particle density:

$$M_F < 0.035 \, P(\Delta h/L) \, \tau w u^2 \quad (7)$$

The value of τw can be obtained most accurately by integrating the depression in brightness across the cloud and assuming the particles are black. The average value of τw in the best image of west plume is ~250 m. Using $u = 15$ m s^{-1}, $\Delta h = 10^3$ m, and $L = 1.5 \times 10^5$ m yields

$$M_F < 10 \text{ kg s}^{-1} \quad (8)$$

for the case that the cloud consists of dark dust particles. If the particles are nitrogen ice crystals the flux limit would be roughly twice this value. As discussed earlier, the mass fraction of ice crystals could be about 5% and so the mass flux of vapor from west plume could be over 400 kg s^{-1}.

The heat of sublimation of solid N_2 is about 2.24×10^5 J kg^{-1}. Therefore, the power required to supply vapor at a rate of 400 kg s^{-1} is about 10^8 W. The solar power incident on Triton is about 1.5 W m^{-2}. Therefore, a solar collector area of about 10×10 km would be required to generate the required vapor if most (say ~2/3) of the solar energy were collected in the greenhouse to drive the process, which would be an exceedingly efficient case.

Assuming the numerous streaks seen on the subliming polar caps were produced earlier in the southern spring and summer by other geyser-like eruptions, we estimate the lifetime of such eruptions must be of the order of a year to several years. If it were much shorter, the probability of witnessing active eruptions would be too small; if it were much longer (comparable to Triton's seasons), more should have been seen.

Given a mass flux for nitrogen vapor as high as 400 kg s^{-1}, an eruption lifetime of 5×10^8 s would suggest a total erupted mass of 2×10^{11} kg. This is equivalent to 0.2 km^3 of nitrogen ice being sublimed during the eruption. For the collector area of 100 km^2 mentioned above, this would imply sublimation of 2 m of solid N_2 over the lifetime of the eruption. These estimates seem high and probably represent upper bounds, as the annual transport of N_2 from pole to pole is only of the order of a meter. Thus, the lower estimates of mass fluxes and lifetimes might be preferable.

REFERENCES AND NOTES

1. On Earth "geyser" denotes a reservoir of liquid water that intermittently erupts due to vapor formation during heating. In contrast, the word "fumarole" is typically restricted to a steam vapor vent where little or no liquid water is present in the reservoir. In this context, planetary geysers would correspond to initial conditions on the low-entropy side of temperature-entropy diagrams, whereas fumarole eruptions would correspond to eruptions from high-entropy conditions [see S. W. Kieffer, in *Satellites of Jupiter*, D. Morrison, Ed. (Univ. of Arizona Press, Tucson, 1982), p. 647]. In a strict thermodynamic sense, the phenomena that we discuss in this report may be fumarolic rather than geyser-like, but because possible models include both direct solid-to-vapor formation as well as liquid-to-vapor eruption, we choose to keep the more commonly used term "geyser." We note that planetary exploration is broadening our use of the terrestrial term "geyser" just as it has expanded our concept of "volcano."
2. B. A. Smith *et al.*, *Science* **246**, 1422 (1989).
3. D. P. Cruikshank, R. H. Brown, R. N. Clark, *Icarus* **58**, 293 (1984); D. P. Cruikshank, R. H. Brown, L. P. Giver, A. T. Tokunaga, *Science* **245**, 283 (1989).
4. R. H. Brown *et al.*, *Science* **250**, 431 (1990); R. L. Kirk *et al.*, *ibid.*, p. 424.
5. E. C. Stone and E. D. Miner, *ibid.* **246**, 1417 (1989); B. Conrath *et al.*, *ibid.*, p. 1454; G. L. Tyler *et al.*, *ibid.*, p. 1466.
6. W. R. Thompson, B. Murray, B. N. Khare, C. Sagan, *J. Geophys. Res.* **92**, 14933 (1987); L. J. Lanzerotti and W. L. Brown, in *Proceedings of the NATO Advanced Research Workshop on Ices in the Solar System* (Plenum, New York, 1984); G. Strazzulla, L. Calcano, G. Foti, *Mon. Not. R. Astron. Soc.* **204**, 59 (1983).
7. R. A. Jacobson, *Astron. Astrophys.* **231**, 241 (1990).
8. A. W. Harris, in *Uranus and Neptune*, J. Bergstralh, Ed. (NASA, Washington, DC, 1984); D. P. Cruikshank and R. H. Brown, in *Satellites*, J. A. Burns and M. S. Matthews, Eds. (Univ. of Arizona Press, Tucson, 1986), p. 836.
9. C. Sagan and C. Chyba, *Nature* **346**, 546 (1990).
10. C. J. Hansen *et al.*, *Science* **250**, 421 (1990).
11. R. V. Yelle *et al.*, *Icarus*, in press.
12. A. P. Ingersoll, *Nature* **344**, 315 (1990).
13. Entropies and enthalpies obtained from integration of heat capacity data in W. F. Giauque and J. O. Clayton, *J. Am. Chem. Soc.* **55**, 4875 (1933).
14. J. S. Turner, *J. Fluid Mech.* **26**, 779 (1966).

Color and Chemistry on Triton

W. Reid Thompson and Carl Sagan

The surface of Triton is very bright but shows subtle yellow to peach hues which probably arise from the production of colored organic compounds from $CH_4 + N_2$ and other simple species. In order to investigate possible relationships between chemical processes and the observed surface distribution of chromophores, we classify the surface units according to color/albedo properties, estimate the rates of production of organic chromophores by the action of ultraviolet light and high-energy charged particles, and compare rates, spectral properties, and expected seasonal redistribution processes to suggest possible origins of the colors seen on Triton's surface.

BEFORE THE VOYAGER ENCOUNTER, spectroscopic measurements and modeling demonstrated the presence of CH_4 (*1, 1a, 2*) and suggested the presence of N_2 (*1a, 3*) on the surface of Triton. The production of simple and complex organic compounds, some white and some possessing yellowish hues, from charged particle and uv processing of mixtures of CH_4 and N_2 in the atmosphere and CH_4, H_2O, and/or N_2 on the surface was expected (*4*). Some quantity of Titan-like haze was also expected, but indications that Triton was probably bright and cold (*2*) suggested that this haze would be thin and the surface would be partially visible provided that N_2 condensate clouds (*5*) were also sufficiently thin.

Voyager observations confirmed the presence of CH_4 and N_2 (*6*) and revealed a very cold surface temperature of about 38 K (*7*) and pressure of about 16 μbar (*8*). The predominantly N_2 atmosphere is in vapor pressure equilibrium with darker portions of the large southern hemisphere cap (SHC) (*9*), while CH_4 is undersaturated, with an atmospheric mole fraction $X_{CH_4} \cong 10^{-5}$ at the surface (*10*). Triton's surface is uniformly very bright (normal reflectance r_n typically 0.6 to 1.0), but has subtle hues which we collectively describe as yellow to "peach" over most of its surface (*11*). Major color/albedo units are obvious to subjective inspection: the apparently permanent SHC extending from the pole to about 15°S has a

surface with relatively dark mottled areas ("splotches"), streaks, and irregular broken areas suggestive of a fragmented surface layer, while a very bright and white transient frost margin extends to and at some longitudes across the equator; this frost overlies a geologically complex equatorial terrain which is darker and more strongly colored than the SHC (*12*).

In this report we use a cluster analysis technique to identify the major spectral units distinguishable in the highest resolution full-disk multiband images of Triton, assess the major chemical processes producing chromophores there, and examine possible relationships between the spectral properties, chemistry, and seasonal cycles.

For color/albedo classification, we use five narrow-angle images of Triton at a phase angle of 39° in the UV, VI, BL, GR, and OR filters which are photometrically calibrated, located on the image frame by limb-fitting, and reprojected to provide a consistent geometry for classification (*13*). The shading due to varying illumination geometry across the disk was removed by an empirical photometric function with parameters determined by least-squares fitting (Table 1). The "normal" albedo r_n is formally equal to A and does not explicitly include phase effects. Because of superior photometric quality and wide wavelength spacing, the quantities R_{UV}, R_{BL}, and R_{OR} computed by dividing the disk intensity point-by-point by the photometric function were used in a three-parameter cluster analysis type of spectral classification (*14*). True color (*15*) and

Laboratory for Planetary Studies, Cornell University, Ithaca, NY 14853.